Available online at www.sciencedirect.com

ScienceDirect

Geochimica et Cosmochimica Acta 222 (2018) 642–654

Geochimica et Cosmochimica Acta

www.elsevier.com/locate/gca

Arsenic uptake in bacterial calcite

Tiziano Catelani [a,b,*], Brunella Perito [c], Francesco Bellucci [a], Sang Soo Lee [d], Paul Fenter [d], Matthew Newville [e], Valentina Rimondi [a], Giovanni Pratesi [a], Pilario Costagliola [a]

[a] *Earth Sciences Dept., Università degli Studi di Firenze, Via G. La Pira 4, 50126 Florence, Italy*
[b] *Electron Microscopy Facility, Fondazione Istituto Italiano di Tecnologia, Via Morego 30, 16163 Genoa, Italy*
[c] *Biology Dept., Università degli Studi di Firenze, Via Madonna del Piano 6, 50019 Sesto Fiorentino (FI), Italy*
[d] *Chemical Sciences and Engineering Division, Argonne National Laboratory, 9700 South Cass Avenue, Argonne, IL 60439, United States*
[e] *GSECARS, University of Chicago, Argonne National Laboratory, 9700 South Cass Avenue, Argonne, IL 60439, United States*

Received 15 March 2017; accepted in revised form 10 November 2017; Available online 16 November 2017

Abstract

Bio-mediated processes for arsenic (As) uptake in calcite were investigated by means of X-ray Diffraction (XRD) and X-ray Absorption Spectroscopy (XAS) coupled with X-ray Fluorescence measurements. The environmental bacterial strain *Bacillus licheniformis* BD5, sampled at the Bullicame Hot Springs (Viterbo, Central Italy), was used to synthesize calcite from As-enriched growth media. Both liquid and solid cultures were applied to simulate planktonic and biofilm community environments, respectively. Bacterial calcite samples cultured in liquid media had an As enrichment factor (Kd) 50 times higher than that from solid media. The XRD analysis revealed an elongation of the crystal lattice along the c axis (by 0.03 Å) for biogenic calcite, which likely resulted from the substitution of larger arsenate for carbonate in the crystal. The XAS data also showed a clear difference in the oxidation state of sorbed As between bacterial and abiotic calcite. Abiotic chemical processes yielded predominantly As(V) uptake whereas bacterial precipitation processes led to the uptake of both As(III) and As(V). The presence of As(III) in bacterial calcite is proposed to result from subsequent reduction of arsenate to arsenite by bacterial activities. To the best of our knowledge, this is the first experimental observation of the incorporation of As(III) in the calcite crystal lattice, revealing a critical role of biochemical processes for the As cycling in nature.

Bacterial calcite; Arsenic; X-ray diffraction; X-ray absorption spectroscopy; As speciation; Travertine

1. INTRODUCTION

Arsenic (As) is a ubiquitous trace element on the Earth crust (Smedley and Kinniburgh, 2002). This element can naturally concentrate in geothermal and groundwater up to 45,000–50,000 μg/l (Smedley and Kinniburgh, 2002). In sediments, geogenic concentration may reach 1000 μg/kg (Costagliola et al., 2010). The occurrence of As can also increase by human activities. The most relevant human activities are mining, metal smelting, combustion of fossil fuels, agricultural pesticide use and production of timber treatments (Matschullat, 2000; Smedley and Kinniburgh, 2002; Murcott, 2012). Soil in mining area may reach As concentration of the order of 10^5 mg/kg (Krysiak and Karczewska, 2007). In soil and natural water environments, sorption of As onto Fe- and Mn oxyhydroxide surfaces is recognized to be a dominant mechanism for As uptake (Raven et al., 1998; Chakraborty et al., 2011). However, a

* Corresponding author at: Electron Microscopy Facility, Fondazione Istituto Italiano di Tecnologia, Via Morego 30, 16163 Genoa, Italy.
E-mail addresses: tiziano.catelani@unifi.it, tiziano.catelani@iit.it (T. Catelani).

https://doi.org/10.1016/j.gca.2017.11.013
0016-7037/

large fraction of these solid phases exist as metastable phases, whose destabilization can release the toxic element back to the ecosystem (Nriagu, 1994; Lenoble et al., 2002; Dixit and Hering, 2003; Sherman and Randal, 2003; Ouvrard et al., 2005; Tufano et al., 2008).

A growing number of studies (Winkel et al., 2013 and reference therein) have been devoted to As trapping in the calcite structure after the pioneering papers of Cheng et al. (1999) and Di Benedetto et al. (2006). Costagliola et al. (2013) argued that calcite could be a more effective sink for a long-term sequestration since As bound in the calcite structure is less mobile than that simply adsorbed onto mineral surfaces (e.g. Fe-Mn oxyhydroxide). The enhanced stability is speculated to result from the incorporation and ordering of As in the calcite lattice, following the substitution of the As oxyanion for CO_3^{2-} in the crystal lattice (Di Benedetto et al., 2006). This substitution leads to a partial distortion of the calcite lattice, usually an expansion of the unit cell along the c axis, due to the size difference between the two anions (Cheng et al., 1999; Román-Ross et al., 2006; Bardelli et al., 2011).

Currently there is no general agreement about the mechanism for this substitution reaction. Alexandratos et al. (2007), Sø et al. (2008) and Yokoyama et al. (2012) claimed that only As(V) can incorporate in calcite. Sø et al. (2008) explained such an effect on the basis of the different chemical behavior of arsenate and arsenite oxyanions. Arsenious acid, H_3AsO_3 having high pK_a values ($pK_a = 9.32$, 12.10, 13.41; Yokoyama et al., 2012), exists predominantly as a neutral species in most natural aqueous conditions (i.e., from acidic to mildly basic solutions), and hence it is likely less reactive to the calcite surface. On the contrary, arsenic acid, H_3AsO_4, that is a stronger acid ($Pk_a = 2.24$, 6.96, 11.50; Yokoyama et al., 2012) than arsenious acid, is present in a dissociated form even at relatively low pH, forming a negative oxyanion that favors As adsorption onto (positively charged) calcite surfaces. This finding has been further confirmed by Yokoyama et al. (2012) who precipitated calcite in presence of solutions containing both As (III) and As(V) showing that almost only As(V) is adsorbed and incorporated in calcite. Natural calcite also generally contains more As(V) compared to As(III), consistent with these laboratory results (Bardelli et al., 2011; Costagliola et al., 2013; Winkel et al., 2013), but with some notable exceptions. Di Benedetto et al. (2006) and Bardelli et al. (2011), on the basis of Electron Paramagnetic Resonance (EPR) and X-ray Absorption Spectroscopy (XAS) measurements, found that natural calcite from travertine deposits of Central Italy prevalently host As(V) but may indeed contain a significant fraction of As(III).

Bardelli et al. (2011) speculated that bacteria could have played an important role in favouring the uptake of As(III) in the calcite lattice. Calcium carbonate precipitation by bacteria is a widespread process, occurring in different taxonomic groups and in different environments (including lakes and hot springs) at a scale ranging from micrometer size bacterial cells to that of meters of rocks (Warren et al., 2001; Perito and Mastromei, 2011). This phenomenon has relevant implications in natural processes and has great potentiality in numerous applications (Dhami et al., 2013; Perito et al., 2014). Different mechanisms of bacterial involvement in precipitation have been proposed and still debated. There is an agreement that the phenomenon can be influenced by the environmental physico-chemical conditions and it is correlated both to the metabolic activity and the cell surface structures of microorganisms (Fortin et al., 1997; Castanier et al., 1999; Perito and Mastromei, 2011). Bacterial calcite precipitation was explored as an alternative trap for As to remediate As contaminated soil by Achal et al. (2012), who found As-calcite co-precipitated products in the bacteria-treated soil. Bacteria also participate in the biogeochemical cycle of elements, especially those with various oxidation states, which can be used as electron donors/acceptors (Konhauser, 2007) to support several metabolic pathways for energy production (Oremland and Stolz, 2003; Lloyd and Oremland, 2006). These reactions, in the case of As (III)-As(V) redox couple, were demonstrated to regulate the As cycling in lakes (Mono Lake, USA; Oremland et al., 2004), mine wastes and water saturated anaerobic soils (Corsini et al., 2010; Weisener et al., 2011).

The aim of this work was to investigate the role of bacteria in driving the Ca-carbonate precipitation and the consequent As trapping in the calcite lattice, in particular whether microbial activity may lead to the incorporation of As(III) into calcite. To do this, we have isolated As-resistant and carbonate-precipitating bacteria from an As-rich environment, the Bullicame hot springs in the northern Latium magmatic province (Italy), where deep hot waters enriched in As (Angelone et al., 2009) reach the surface, precipitating travertines. In these travertines, variable concentrations of As (39–279 mg/kg) were prevalently bound (about 95%) to calcite (Di Benedetto et al., 2011). Among bacteria isolated from the Bullicame hot waters potentially able to trap As into calcite, we selected one strain for its ability in precipitating Ca-carbonate in presence of As in laboratory conditions. Biogenic and synthetic calcite obtained in presence of As were then compared by means of X-ray Diffraction (XRD), X-ray Fluorescence (XRF) and X-ray Absorption Spectroscopy (XAS) analyses. Moreover, we explored how the calcite chemistry can affect the As uptake by adding Mg to the solution where calcite was grown.

2. EXPERIMENTAL PROCEDURES

2.1. Sampling area

The thermal area of Viterbo (Northern Latium, Central Italy) is composed by several hot springs (“Carletti Pool”, “Zitelle”, “Bagnaccio”, “Masse di San Sisto” and “Bullicame”), all located in a small and well defined area (Fig. S1), usually referred to as the “Bullicame” thermal field (Di Benedetto et al., 2011). The physical and chemical properties of the water at Bullicame, as well as the mineralogical and chemical characteristics of the travertines precipitated by the thermal waters, have been described with some detail by Angelone et al. (2009) and Di Benedetto et al. (2011). At the spring, water had a temperature of 57 °C, a pH of 6.5 and a conductivity of 2.75 mS. The

hot springs contain variable concentrations of As (typically 300–400 μg/l) in agreement with Angelone et al. (2009), with higher As contents (up to 1 mg/l) at the Bullicame hot spring. All the hot springs show clear signs of biological activity with microbial mats onto and below the surface of recent travertines (Fig. S1c).

2.2. Water sampling, bacteria isolation and identification

Two water samples from the hot spring Bullicame, one near the edge and the other near the center of the spring, were collected into sterile glass bottles and immediately brought to the laboratory. Each water sample was filtered through 0.2 μm Millipore filter, and then the microbial cells trapped onto filter were collected by washing filters with the filtered water. Small volumes (0.1 ml) of undiluted and serially diluted cell suspensions were plated on Nutrient Agar (NA) As-enriched (As-en NA) by adding to the NA medium (OXOID; typical formula (g/l): 'Lab-Lemco' powder 1.0, Yeast extract 2.0, Peptone 5.0, Sodium chloride 5.0, Agar 15.0; pH 7.4 ± 0.2 at 25 °C) 1/10 volume as Bullicame filtered water, and incubated up to two weeks at 57 °C. Growing colonies were observed at the stereomicroscope and classified on morphology. For each morphotype, some strains were streaked and then isolated on As-en NA.

The selected strain BD5 (see RESULTS), was identified by means of rDNA analysis. Genomic DNA extraction, PCR conditions, purification and sequencing of the amplified 16S rRNA gene were carried out as described in Marvasi et al. (2009). The newly generated 16S gene sequence was deposited at the NCBI database under the accession number KY765937. Highly similar sequences were searched by BLAST at the NCBI database (http://www.ncbi.nlm.nih.gov).

2.3. Biogenic calcite precipitation

Sixty-five bacterial strains as representatives of different morphotypes were selected and tested for calcite production by streaking them on solid B4 precipitation growth medium (0.4% yeast-extract, 0.5% dextrose, 0.25% calcium acetate, 1.5% agar if solid, buffered at pH 8). *Bacillus subtilis* 168 was used as calcite producing control strain (Barabesi et al., 2007). From literature we knew that in the superficial environment As(III) is readily oxidized to As(V); in fact in travertine calcite As is mainly as As(V) (Angelone et al., 2009; Costagliola et al., 2013; Winkel et al., 2013). In order to compare our results with natural travertines, we planned to perform all the experiments in a normal atmosphere using an As(V) standard solution. Therefore, the bacterial strains showing faster growth and appreciable amounts of precipitates were sequentially selected by streaking them on solid B4 medium with increasing As content up to 10 mg/l. The B4 As-enriched medium (As-enB4) was obtained by progressively adding a filter sterilised As solution (H_3AsO_4 standard solution 1000 mg/l [Merk]) to B4 up to 10 mg/l (As-enB4). All the subsequent analyses on bacterial calcite were carried out on carbonates produced by the selected strain called BD5 (see RESULTS) in As-enB4 medium added with As 10 mg/l, a suitable condition to produce calcite having an easily detectable amount of As for XRF and XAS studies.

Moreover, strain BD5 was grown both in liquid and solid B4 medium. We used these two phases of the B4 medium in order to investigate calcite precipitation by bacteria growing in different lifestyles, namely as planktonic cells in liquid medium and as a biofilm community on solid medium (Fig. S2). This would allow to understand if bacteria lifestyle could affect calcite precipitation and As uptake process, and partly resemble different natural environments.

Bacterial cultures in As-enB4 were incubated at 57 °C for 2 weeks on solid and for 4 weeks in liquid media. Calcite production was monitored visually by observing the growth of calcite crystals in solution and through a stereomicroscope on solid media (See Supporting Files; Fig. S2). Calcite precipitation takes place as a result of the bacterial respiration pathway which consists in the oxidation of organic compounds from the growth media. Such process produces CO_2 and, consequently, an increase of carbonic acid species in the medium. Because of the buffered, alkaline environment, and the presence of cations as Ca and Mg, carbonates are readily precipitated in the growth medium (Konhauser, 2007). As a control experiment, liquid and solid B4 without bacterial cells were also incubated; no precipitates were observed until the end of incubation, confirming the biological origin of the calcite. At the end of the incubation period, carbonates from solid culture media were collected by scraping the bacterial streaks from plates and washing them several times in distilled water until the suspension appeared clear. Liquid cultures were similarly clarified by several washing steps. Then suspensions were filtered on Whatman grade 5 cellulose filters and subsequently dried. Carbonate samples cultured in solid and liquid media (SCC and LCC, respectively) were obtained from BD5 culture in As-enB4.

In order to investigate the lattice strain by Mg-Ca substitution in calcite crystals and its effect on As uptake, we replicated the experiments using As-enB4 media modified by adding Mg (by means of Mg-acetate). The Mg/Ca molar ratio was maintained below 0.02 to prevent dolomite precipitation. Carbonate samples SCC-Mg and LCC-Mg were obtained from BD5 culture in Mg enriched As-enB4 solid and liquid media, respectively. Finally, an As- and Mg-free standard sample (namely SCC-CTR) was produced by growing BD5 in an unmodified B4 medium. Details about bacterial carbonate samples are reported in Table 1.

2.4. Reference material collection, production and analysis

A set of reference calcite samples was prepared for comparison purposes.

The first one was prepared from a collection of both fossil and presently-forming travertines. Fossil travertines were sampled at the Bullicame area (samples BL4, BL5, BL7) and in the Pecora Valley district (Southern Tuscany, Italy; cfr. Costagliola et al., 2010, 2013; Bardelli et al., 2011; sample TRSE). Presently forming travertines were all sampled at Bullicame Hot Springs (samples BL1, BL2, BL3) and Zitelle Hot Spring (ZIT).

Table 1
List of biological carbonates produced by *B. licheniformis*, Bullicame travertines and As-bearing synthetic calcites. As concentration was measured by means of XRF for biogenic calcite and ICP-OES for the other materials.

Sample	Description	As (mg/kg)	As solution (mg/l)	Kd (l/kg) $[As]_{CAL}/[As]_{LIQ}$
SCC-Mg	Biogenic, solid culture medium As-en B4, Mg/Ca < 2%	43	10	4.3
SCC	Biogenic, As-en B4solid culture medium	27	10	2.7
LCC-Mg	Biogenic, As-en B4 liquid culture medium, Mg/Ca < 2%	1381	10	138
LCC	Biogenic, As-en B4 liquid culture medium	1053	10	105
SCC-CTR	Biogenic, B4 solid culture medium, No Arsenic	–	–	–
BL1	Now-forming travertine, Bullicame (VT), Italy	154	1	154
BL2	//	206	1	206
BL3	//	201	1	201
BL4	Fossil travertine, Bullicame (VT), Italy	160	1	160
BL5	//	185	1	185
BL7	//	123	1	123
ZIT	Travertine Zitelle Hot Spring (VT) Italy	91	0.58	157
TRSE	Fossil travertine, Pecora River Valley, Italy	110	–	–
RR5	Synthetic calcite	169	74.9	2.2
RR5Mg2	Synthetic calcite, Mg 2%	419	74.9	5.6
RR3	Synthetic calcite	2.3	74.9	0.03

A second set of reference samples was prepared by precipitating abiotic As-bearing calcite (samples RR3, RR5 and RR5Mg2), following the procedure by Romàn-Ross et al. (2006). Briefly, the abiotic calcite was precipitated by mixing a 100 ml 0.5 M Na_2CO_3 solution containing 1 mM As (~75 mg/l), buffered at pH 8.9 with NaOH, with a 0.5 M $CaCl_2$ solution, added drop by drop for 1 h, while stirring. Magnesian calcite was produced by adding both 0.5 M $CaCl_2$ and $MgCl_2$ solutions, maintaining the Mg/Ca molar ratio <0.02. Sodium arsenate dibasic heptahydrate, $Na_2HAsO_4{\cdot}7H_2O$ (Sigma Aldrich), and arsenious acid, H_3AsO_3, in nitric acid solution 0.1 N (Merk) were used as As source for As(V) (RR5, RR5Mg), and As(III) (RR3), respectively. In order to avoid any As(III) oxidation, the As(III)-bearing calcite RR3 was precipitated in an oxygen-free chamber (O_2 < 1 ppm).

The As concentration was determined by means of Inductively Coupled Plasma – Optical Emission Spectroscopy (ICP-OES) analysis (Perkin Elmer Optima 8000; As detection limit 1.0 µg/l) after calcite acid digestion in "aqua regia" ($HCl + HNO_3$) in microwave oven (CEM Mars-5 microwave mineralizer) of 0.5 mg of ball-milled sample. Compositional results are the mean of three different measurements. A complete list of the reference samples and their details are reported in Table 1.

2.5. Scanning Electron Microscopy (SEM) imaging

The morphology, texture, and crystallinity of bacterial calcite samples were investigated by means of Scanning Electron Microscopy (SEM) analysis (ZEISS EVO MA15, operating at 10 kV acceleration voltage), using both Secondary Electrons (SE) and Backscattered Electron (BSE) imaging (Fig. 1). In order to better appreciate the calcite development onto bacterial cells, we cultured strain BD5 (see RESULTS) up to 30 h of incubation in liquid As-enB4 medium in bottles where sterile flat cleaved inorganic calcite crystals (from Mina Prieta Linda, Naica, Chihuahua, Mexico) at the bottom were used as a holder for bacterial growth (Fig. 2). Samples for SEM imaging have been taken directly from the cultures, washed, dried and carbon-coated, without any specific processing.

2.6. XRD, XRF and XAS measurements

Biological calcite samples, after washing and milling, were analyzed for their mineralogical composition by XRD. Because of the slight amount of biological calcite produced by bacterial cultures, As concentration in biogenic calcites was carried out by means of XRF – instead of ICP-OES – in order to preserve material for further analyses. XAS and XRF samples were prepared in the same way: biogenic calcites were milled and pressed in 3 mm thick punched plastic holders and enclosed with 0.2 mm thick polyimide film tape.

– XRD

XRD measurements were performed with Philips PW 1050/37 X-ray powder diffractometer (Earth Sciences Dept., University of Florence), operated with a Cu anode, a graphite monochromator and with a PANalytical X'Pert PRO data acquiring system. The filament current of the tube was 20 mA and the acceleration potential 40 kV. A thin layer of milled biogenic carbonates was applied on a silicon wafer, and X-ray diffraction pattern was recorded from 8° to 120°, with a step spacing of 0.2° measured for 0.1 s. Yttrium oxide (Y_2O_3) was used as a reference material. All data were analyzed with GSAS-EXPGUI (Toby, 2001) software to refine cell parameters and phase amounts (weight %). Spectra relative to biogenic calcite are reported in the Supporting Files (Fig. S3).

– XRF

XRF measurements were performed with WD-XRF Rigaku PrimusII (CRIST – Structural Crystalchemistry Interdepartmental Center, University of Florence),

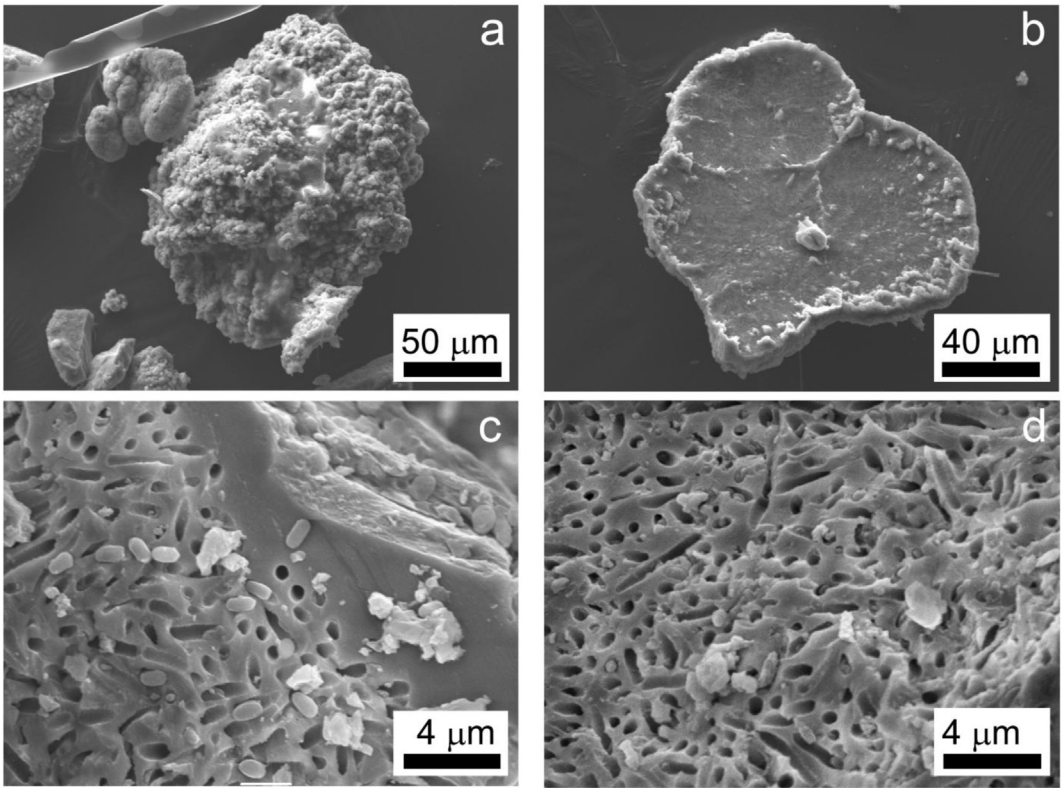

Fig. 1. SEM-SE images of isolated calcite concretions produced by *B. licheniformis* grown on B4 solid medium (a, b). Cross section of freshly milled calcite exhibits a "Swiss Cheese" structure both in solid (c) and liquid (d) bacterial cultures.

equipped with a Rh X-ray source and Silicon monochromator. Biogenic carbonates were held between polyimide film tapes in punched ($2 \times 4\ mm^2$, 1.5 mm thick) holders. Fluorescence signals were measured from each sample using 1 mm^2 spot repeated four times on the sample surface.

As reference materials for instrument calibration were used some travertines from Bullicame Hot Springs (Table 1), previously analyzed by means of ICP-OES to get As concentration. The As contents in these samples ranged from 10 to 206 mg/kg while the host rock was mostly made of $CaCO_3$. Eight standards produced by mixing As_2O_5 (Merk) in a pure $CaCO_3$ powder (Merk) were used for the calibration of samples with higher As contents (from 300 to 3000 mg/kg).

– XAS

Bulk X-ray absorption spectroscopy (XAS) experiments on the As K-edge were performed at 13-BMD beamline (GeoSoilEnviroCARS) at the Advanced Photon Source (APS), Argonne National Laboratory (ANL – Argonne, IL). The K-edge X-ray absorption near-edge structure (XANES) spectra were collected in fluorescence mode from −150 to 640 eV with 5 eV steps before the main edge (11871.5 eV for As(V); 11868 eV for As(III)), 0.25 eV steps across the main edge (from −15 eV to 25 eV), and steps in electron wavenumber of 0.05 $Å^{-1}$ above the edge, with the energy selected with a Si(111) monochromator. Samples were held between polyimide film tapes in punched plastic holders (as described for XRF measurements), mounted in the X-ray beam at a 45° angle. X-ray fluorescence was recorded using a 13 element Ge solid-state array multi-element detector and the incident beam intensity (I_0) was recorded using a standard ionization detector. Energy calibration was performed by assigning the K-edge energy of As(V) (11871.5 eV) and As(III) (11868 eV) of six standard materials: arsenic oxide (As_2O_5), scorodite ($Fe^{3+}AsO_4{\cdot}2H_2O$) and schneiderhöhnite ($Fe^{2+}Fe^{3+}_3[As_5O_{13}]$), arsenious oxide ($As_2O_3$), calcium arsenate ($Ca_3(AsO_4)_2$) and sodium arsenate ($Na_2HAsO_4{\cdot}7H_2O$). For extended X-ray absorption fine structure (EXAFS) measurements, multiple scans (from 3 to 12 depending on As contents) were collected on each sample and merged to increase the signal to noise ratio. Data were corrected for detector deadtime, and the analysis was performed with Athena XAS data processing software, Demeter Pack (Ravel and Newville, 2005).

3. RESULTS

3.1. Characterization of the bacterial strain BD5 and its precipitation product

Among the bacteria isolated from Bullicame hot spring, strain BD5 showed the best precipitation potential (Fig. S2d), and was then selected for further characterization. Sequence analyses of 16S rDNA showed a 98% identity with the 16S rDNA of *B. licheniformis* DSM13. The

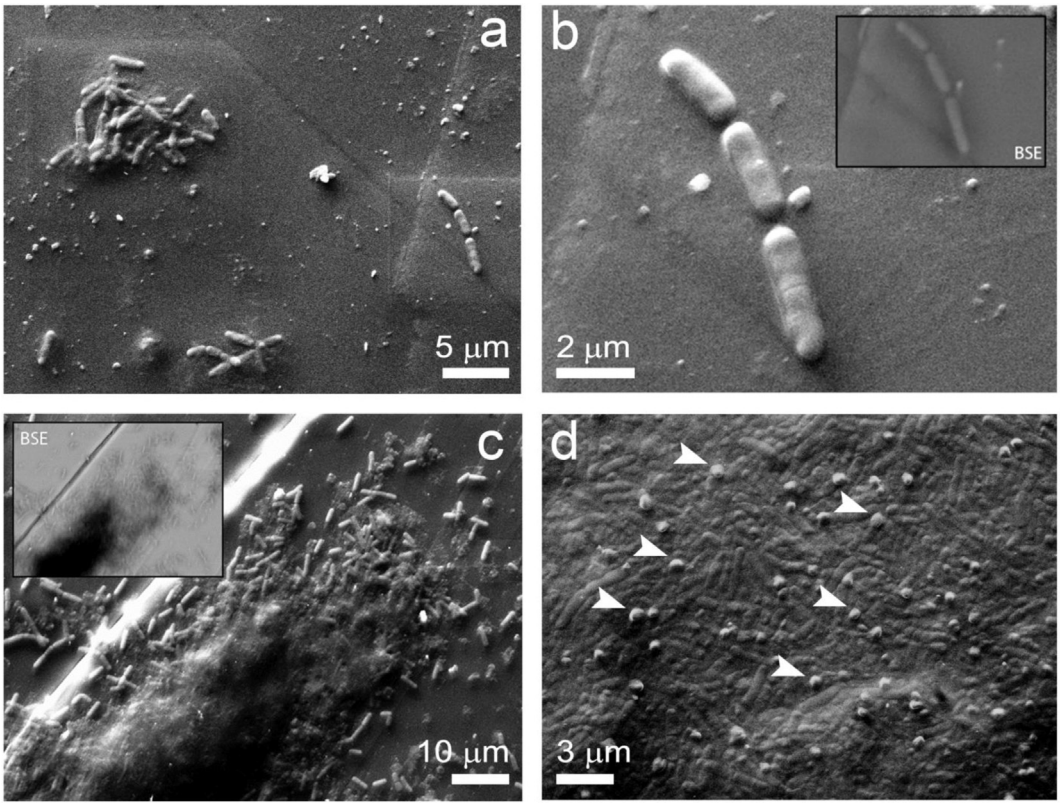

Fig. 2. *B. licheniformis* BD5 growth and calcite production onto inorganic calcite surfaces in B4 liquid medium observed at SEM-SE: after 3 h of incubation (a), bacterial cells appear in short chains and small aggregates adherent to the surface. A detail of the same sample (b) shows a short chain of three rod-shaped cells (in the inset the SEM-BSE imaging); after 7 h of incubation (c), bacterial biofilm appears more developed. The SEM-BSE image shown in the inset underlies the wide extracellular polymeric matrix (black area); after 30 h of incubation (d), the bacterial mat completely covers the calcite surface. Several endospores are visible as white dots (highlighted with white arrows).

BD5 cells had morphology of a rod spore-forming bacterium as observed under the optical microscope and SEM (Fig. 2), which fitted with the molecular classification. Calcite produced by BD5 on solid As-enB4 formed clusters about 200 μm in diameter. The SEM images showed that these clusters were composed of fine-grained anhedral calcite particles (Fig. 1a and b). Crust cross-sections showed an internal "Swiss cheese" structure with the presence of many internal cavities about 1 μm in diameter lodging bacterial bodies (Fig. 1c and d). Such a structure indicated that calcite forms onto bacterial cells surface and bacteria get embedded into the calcite they produce, as known in literature (Castanier et al., 1999).

The production of calcite during bacterial growth onto an inorganic calcite surface was observed by SEM at different elapsed times (up to 30 h) of incubation (Fig. 2). After 3 h of incubation, BD5 bacterial cells appeared in short chains and small aggregates deposited onto the inorganic calcite surface (Fig. 2a). In the following hours, the bacterial biofilm progressively developed until it covered the whole calcite surface to produce a thicker extracellular polymeric substance (EPS) matrix entrapping cells (Fig. 2c and d). By SEM-BSE images bacterial cells appeared covered by a calcite envelope after 3 h of cultivation, as shown by the low compositional contrast with the calcite support (Fig. 2b). The growth of a thick biofilm was evident by the presence of a wide dark area on the brighter calcite substrate (Fig. 2c).

3.2. Mineralogical composition

XRD analyses revealed that the biogenic carbonates produced in liquid culture were a mixture of calcite and vaterite, whereas carbonates precipitated in a solid culture were mainly calcite (Table 2). The amounts of vaterite, calculated by means of the Rietveld analysis were about 8 wt.% in LCC-Mg and 40 wt.% in LCC (Table 2). The biogenic carbonates SCC-Mg and SCC, produced in the solid growth medium, in addition to the calcite XRD pattern exhibit a weak but distinct peak at about 3.5 Å, which does not match the Bragg peaks of any $CaCO_3$ polymorphs. Finally, XRD data show no Mg-carbonate phase in appreciable quantities in any sample (Fig. S3).

The results reported in Table 2 clearly indicate that LCC-Mg and LCC (produced in liquid media) exhibit larger cell lattice constants and volume: c-lattice constants – 17.0910 Å and 17.0988 Å respectively – are about 0.02–0.03 Å longer than those for the other bacterial calcite samples. In fact, calcite in SCC owns lattice constants (17.0664 Å) similar to those for calcite both reported in literature (e.g., Graf, 1961; Markgraf and Reeder, 1985) and in the As-free SCC-CTR (17.0765 Å). In contrast, SCC-Mg

Table 2
Mineralogical composition and refined reticular constants of biological calcite.

Sample	Phases	Phase ratio (wt.%)	Calcite reticular constants (Å)			Cell volume (Å^3)
			a	c	c/a	
SCC-Mg	Calcite	–	4.9765 (0.0001)	17.0506 (0.0006)	3.426	365.709 (0.023)
SCC	Calcite	–	4.9848 (0.0002)	17.0664 (0.0007)	3.424	367.253 (0.032)
LCC-Mg	Calcite	91.7%	4.9903 (0.0004)	17.0910 (0.0014)	3.425	368.597 (0.072)
	Vaterite	8.3%				
LCC	Calcite	60.8%	4.9916 (0.0005)	17.0988 (0.0022)	3.425	368.951 (0.077)
	Vaterite	39.2%				
SCC-CTR	Calcite	–	4.9858 (0.0001)	17.0765 (0.0009)	3.425	367.63 (0.02)
Calcite (Markgraf and Reeder, 1985)			4.988	17.061	3.420	367.6

exhibits a smaller c-lattice constant: 17.0506 Å than the other samples. Biogenic calcites containing Mg (SCC-Mg and LCC-Mg) exhibit smaller c-lattice constants than their corresponding Mg-free samples SCC and LCC.

3.3. As uptake in biogenic carbonates

XRF measurements performed on the biogenic carbonates and the reference materials are reported in Table 1. The biogenic calcites produced in solid culture media have 27 (SCC) and 43 (SCC-Mg) mg/kg of As, substantially lower than 1053 (LCC) and 1381 (LCC-Mg) mg/kg for the samples produced in the liquid media, although the initial As concentration in the growth medium was the same (10 mg/l). As a comparison, the calcite composing of the travertines from Bullicame Hot Springs and Pecora Valley exhibits As concentrations ranging from 91 to 206 mg/kg.

The apparent distribution coefficient, Kd (l/kg) was calculated on the basis of the As concentration in precipitated carbonates (mg/kg) with respect to the As concentration (mg/l) in the initial solution (Yokoyama et al., 2012). We found a value of Kd of about 10^2 (138 and 105 for LCC-Mg and LCC) for biogenic calcite produced in the liquid culture media. Similar Kd values (from 123 to 206 l/kg) were found for travertines at the Bullicame Hot Springs. In contrast, bacterial calcite produced in the solid As-enB4 culture media (SCC-Mg and SCC) had much lower Kd values: 2.7 and 4.3 l/kg. The Kd values for samples LCC-Mg and LCC were similar notwithstanding the different mineralogical composition (8 wt.% against the 40 wt.% of vaterite).

3.4. As speciation in biogenic carbonates

The XANES spectra (Fig. 3a and b) reveal that As sorbed in biogenic samples can have different oxidation states depending on their culture media (liquid or solid). Samples LCC-Mg and LCC, both from liquid culture media, exhibit only As(V). On the contrary, biogenic samples produced in solid culture media (SCC-Mg and SCC) contain both As(V) and As(III). This feature is evident in Fig. 4 where the XANES spectra were fitted by means of a linear combination of two standards' spectra: schneiderhöhnite for As(III) and scorodite for As(V). This analysis indicates that the As(III):As(V) ratio was about 1:4 for

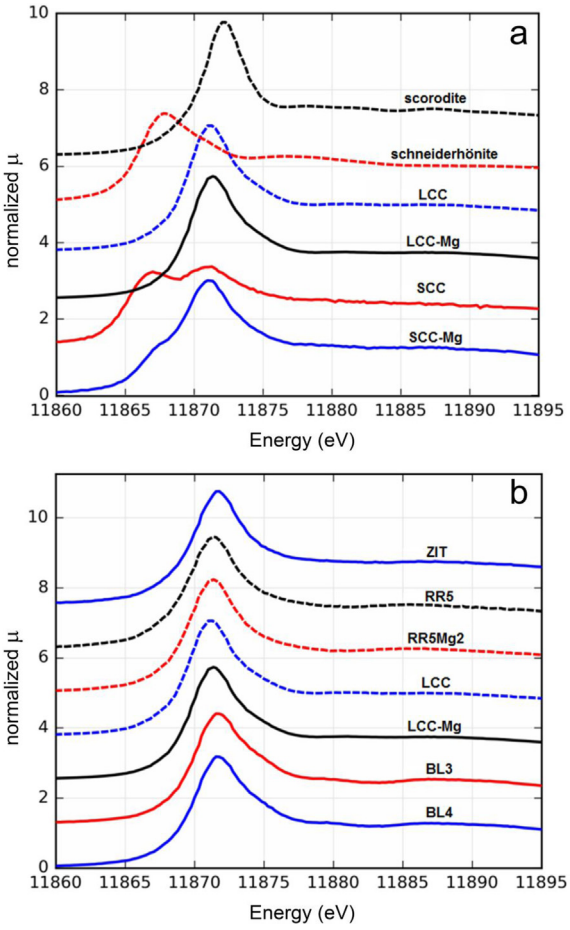

Fig. 3. X-ray As K-edge absorption spectra of bacterial calcite samples cultured both in liquid (LCC and LCC-Mg) and solid culture media (SCC and SCC-Mg) compared with two standard samples for As(V) (scorodite) and As(III) (schneiderhönite) (a) and XAS spectra of bacterial calcites precipitated from liquid medium (LCC and LCC-Mg) compared with Bullicame Hot Springs Travertines (BL3, BL4, ZIT) and synthetic calcites (RR5, RR5Mg2) (b).

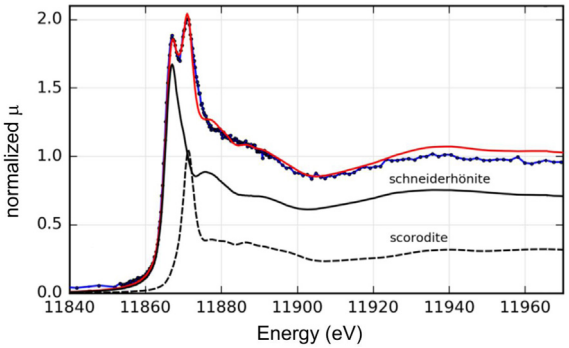

Fig. 4. Least squares fit (red line) of BR2 XAS spectrum (blue) using a linear combination of the scorodite (solid black) and schneiderhönite (dotted black) spectra. (It is important to underlie that these spectra are used for peak deconvolution, but it does not imply that these phases are actually present in the studied samples.) (For interpretation of the references to colour in this figure legend, the reader is referred to the web version of this article.)

SCC-Mg and 2:1 for SCC. The ratio for an abiotic calcite RR3 was about 2:1. While this sample was prepared using concentrated arsenious acid, a partial oxidation from As (III) to As(V) occurred during the dilution process with water which likely contained a small amount of dissolved oxygen. In comparison, natural As-bearing travertines (both contemporary and fossil Bullicame Hot Spring travertines) contained only As(V), similar to biogenic samples produced in liquid culture media.

The similarities between LCC-Mg and LCC, and Bullicame travertines are evident in both the XANES and EXAFS regions (Fig. 5), which is diagnostic to understand if As is adsorbed or co-precipitated with calcite (Winkel et al., 2013). On the basis of XANES spectra, As(V)-bearing calcite samples could be divided in two groups: in the first case (adsorption) a broad band occurs close to the As(V) K absorption edge (11871.5 eV), while in the other case (co-precipitation) a shoulder is present at about +8 eV and two features at +15 eV and +20 eV, respectively. ZIT and TRSE travertines (from Zitelle Hot Spring and Pecora Valley, respectively; Table 2) belong to the first group, having a spectrum very similar to the abiotic calcites RR5 and RR5Mg2. The Bullicame travertines (here only BL3 and BL4 are reported; Fig. 3b) exhibit the features of the second group, just like the other travertines from Bullicame Hot Spring (spectra not reported). Finally, the biogenic calcite LCC-Mg and LCC have intermediate spectra: they exhibit not only a weak feature close to the absorption edge, similar to the shoulder in the travertines spectra, but also a broad band in the region +15 eV and +20 eV (Fig. 3b).

These features are more evident in k-space EXAFS spectra (Fig. 5a). Bullicame travertines (BL) exhibit a clear split of the 4.8 $Å^{-1}$ band and a small shoulder at 6.3 $Å^{-1}$, while ZIT, TRSE, synthetic calcites (RR5 and RR5Mg2) and biogenic calcites (LCC-Mg and LCC) only exhibit a single frequency oscillation. The radial distribution functions (Fig. 5b) show no distinct peaks at R > 2 Å (values not corrected for phase shift). Finally, the biogenic SCC exhibits a

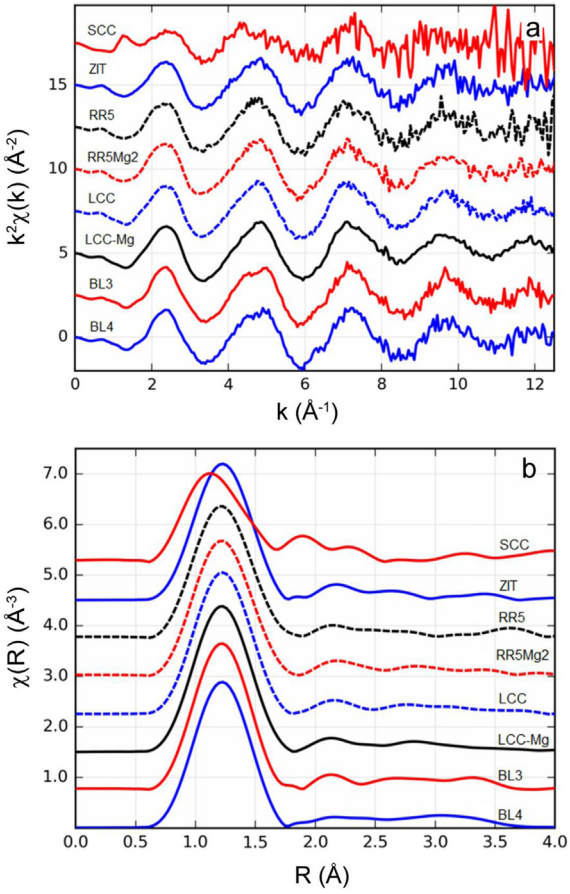

Fig. 5. XAS $k^2\chi(k)$ (a) and Fourier transformed XAS χ(R) (b) of bacterial calcites precipitated from liquid (LCC and LCC-Mg) compared with Bullicame Hot Springs Travertines (BL3, BL4, ZIT), synthetic calcites (RR5, RR5Mg2), and solid medium cultured As(III)-bearing SCC.

clear combination of peaks in the range 1 Å < R < 2 Å, corresponding to different first-coordination shells for the two different oxidation states As(III) and As(V) (Fig. 5b).

4. DISCUSSION

Data on As trapping by bacterial calcite precipitation reported in this work come from a study on the strain BD5 of *B. licheniformis* isolated from the Bullicame hot springs. *B. licheniformis* is a spore-forming bacterium commonly found in soil, known to be an As tolerant bacterium (Tripti and Shardendu, 2016) and to be able to precipitate calcium carbonate (Vahabi et al., 2013), and with a high potential for biotechnological applications (Veith et al., 2004). Strain BD5 resulted in a fast precipitation of calcite in a suitable medium (calcite was present onto bacterial cell surfaces after 3 h of cultivation, Fig. 2) entrapping both As (III) and As(V) in the growing calcite.

Our results clearly indicate that the nature (liquid vs solid) of the bacterial growing media strongly influences the carbonate mineralogy. A solid medium favors the precipitation of calcite over other calcium carbonate poly-

morphs, whereas liquid medium triggers the precipitation of both calcite and vaterite. This result is not surprising since it is known that vaterite is a common product of the biological activity during carbonate precipitation from liquid solutions (Warren et al., 2001). Yokoyama et al. (2012) observed that, under abiotic conditions, a low percentage (at most 5%) of vaterite was present during calcite precipitation from supersaturated solution in the pH range 9–11, and the amount decreased with aging of the sample until 54 h, when all vaterite was converted to calcite. Ogino et al. (1987) reported that vaterite is a metastable phase which exists as a precursor of calcite, during its precipitation from $CaCO_3$ supersaturated solutions. However, our samples maintained significantly higher contents (up to almost 40% in LCC) of vaterite than previously reported (Yokoyama et al., 2012).

It is reported in literature that vaterite to calcite conversion may be hindered by the sorption of ions (Kamiya et al., 2004; Yokoyama et al., 2012). Adsorption of As oxyanions can either inhibit the vaterite-calcite transformation by lowering the Gibbs free energy of vaterite surfaces or increase the vaterite lifetime by increasing the activation energy for the reaction (Yokoyama et al., 2012). Moreover considering that in the present study the biological samples in the liquid culture media were produced in 4 weeks, our results suggest that under high As concentrations, like those adopted in our experiments, the biological process of $CaCO_3$ precipitation extends the vaterite lifetime with respect to abiotic $CaCO_3$ precipitation.

It is not well known if a critical concentration of As for the inhibition vaterite-calcite transformation exists. Winkel et al. (2013) reported of travertines with ~1000 mg/kg As, precipitated from solutions containing 3700 μg/l As, with no evidence of vaterite. Equally, travertines from the Bullicame area, even the recent ones showing evident signs of biological activity, are mainly made up of calcite with minor aragonite occurrence (Di Benedetto et al., 2011). This comparison suggests that an extended aging under ambient conditions may lead to a continuous vaterite-calcite transition.

In terms of the reactivity, it was not possible to determine separately the Kd value for vaterite from that for calcite because these two phases were intrinsically mixed in each sample. However, our data show that the As concentration (and thus Kd) was generally similar to one another despite a wide range of vaterite contents. This similar As uptake implies that the Kd value for vaterite may be similar to that for calcite.

The measured As contents as well as the Kd values showed that the effectiveness of As uptake by calcite strongly depends on the bacterial activity. From the results reported above, it could be observed that commensurate As concentrations and Kd values are obtained for the biogenic calcite prepared in a liquid medium with those observed at Bullicame hot springs. Conversely, both the As concentrations and Kd values of calcite samples produced on a solid medium were significantly lower than those observed for the Bullicame travertines. Since the initial concentrations of As in these growing media were the same (10 mg/l), an explanation for these differences could be different diffusion rates and availabilities of As in the growth media (liquid vs solid). In the liquid media, the diffusion of As is conceivably rapid enough to replenish the depletion caused by the As uptake in the calcite and/or vaterite growing onto the bacterial cells, but the same process could be hindered in the solid medium. Namely, planktonic cells growing in liquid medium have more chance to get As from solution than bacteria growing onto solid medium surface from biofilm matrix. In conclusion, the diffusion of As into the medium may be the critical parameter that controls the As uptake in calcite. Besides this effect, As speciation could affect the final Kd for biogenic calcite grown in liquid and solid cultures: in fact Kd for As(III) is estimated to be about 2000 times smaller than As(V) (Yokoyama et al., 2012). As debated below, solid cultured calcite samples have both As(III) and As(V), suggesting that under particular conditions As(III) is allowed to sink in calcite but at the same time it reduces the overall As uptake.

Our results also denote another interesting insight: even a small amount of Mg in the growth media can drastically increase the uptake of As(V) from the solution. We clearly observed an increase of As in biogenic calcite samples precipitated in both the solid and liquid culture media. Namely, Mg-bearing calcite samples, SCC-Mg and LCC-Mg, exhibit an increase of As content by about 59% and 33% with respect to the Mg-free SCC and LCC. This trend is also confirmed for abiotic samples (RR5 and RR5-Mg2). This Mg effect on As uptake in calcite has not been studied systematically although Mg is used frequently as an additive for promoting the growth of arsenical calcite (Fukushi et al., 2011 – US patent 8227378; Costagliola et al., 2013). The positive effect (higher Kd) of Mg on the As uptake could be explained by steric effect. Isomorphic substitution of smaller Mg^{2+} (with an ionic radius of 0.72 Å) for bigger Ca^{2+} (with an ionic radius of 0.99 Å) leads to shrinking of the octahedral site as demonstrated by EXAFS studies of Mg-O and Ca-O bond lengths in the calcite structure (Finch and Allison, 2007). As a consequence, the Mg-Ca substitution provides more space for the replacement of larger As oxyanions for carbonate ions (Bardelli et al., 2011). Besides this crystallographic explanation it is reasonable to consider the role of Mg in calcite precipitation which could affect As uptake. In particular, some studies (Han and Aizenberg, 2003; Astilleros et al., 2010) showed how Mg in the precipitating solution can decrease the precipitation rate of calcite from solution and affect the crystal size and morphology.

Biogenic calcites with higher amounts of As (LCC-Mg and LCC) clearly exhibit increased c-lattice constants, which is consistent with previous observations of the elongation of the c-axis due to the substitution of either pyramidal As(III) or tetrahedral As(V) for a planar carbonate ion (Cheng et al., 1999; Román-Ross et al., 2006; Di Benedetto et al., 2011), although we point out that Winkel et al. (2013) reported no changes in the crystal lattice in As-bearing calcite in travertine rocks. For relatively high As concentrations (samples LCC-Mg and LCC) such effect is significant with an increase of the c-axis length in As-bearing calcite by ~0.03 Å with respect to As-free calcite. In contrast, biogenic calcite with low As contents (e.g.

SCC) shows lattice constants similar to non-biogenic As-free calcite (Markgraf and Reeder, 1985) and biogenic As-free calcite SCC-CTR, suggesting no unit-cell expansion along the c axis in low As concentrations. It is noteworthy that a c-axis expansion was observed by Di Benedetto et al. (2011) in calcites from the Bullicame Travertines (Carletti Pool). These Authors proposed, accordingly to Pokroy et al. (2008) and Zolotoyabko et al. (2010), that biogenic calcite, such as those at Bullicame, often shows an elongated c-axis due to the presence of an organic layer placed perpendicularly to the c-axis. Therefore, the organic matter could concur in expanding the c-axis, while an opposite effect could be imputed to the Mg-Ca substitution: in fact, Mg-bearing calcites SCC-Mg and LCC-Mg have correspondingly shorter c-axes than Mg-free SCC and LCC. Such effect could be related to the shorter ionic radius of Mg (0.72 Å) with respect to Ca (0.99 Å), in agreement with literature (Paquette and Reeder, 1990).

XAS data indicate that the Bullicame travertines, synthetic calcite and biogenic carbonates produced in liquid culture media contain exclusively As(V). This observation confirms the results obtained in recent literatures (e.g., Alexandratos et al., 2007; Sø et al., 2008; Bardelli et al., 2011; Yokoyama et al., 2012) although Bardelli et al. (2011) report the presence of As(III) oxyanions in travertine (composed mostly of calcite) samples from the Pecora River Valley (Southern Tuscany, Italy). In contrast, the As K-edge XANES analyses clearly indicate that biological carbonates precipitated from solid culture media host As(III) in addition to As(V). The As introduced in the culture media was only As(V) and all bacteria cultures and measurements on the biogenic products were carried out in aerobic conditions, so a reduction process occurred during incubation.

It seems clear that, because the As(V)/As(III) oxidation/reduction potential ranges from +60 to +135 mV (Lloyd and Oremland, 2006), the As(V) reduction to As(III) was performed by bacteria. It is well known that bacteria can reduce As(V) following two main pathways: (1) the dissimilatory reduction to As(III) carried out by bacteria able to respire arsenate coupling the reaction with the oxidation of organic matter; (2) the As(V) reduction pathway to As (III) via the ArsC system (Oremland and Stolz, 2003), which is a mechanism of detoxification and resistance. The arsenate-reductases involved in these two pathways are different (Oremland and Stolz, 2003; Silver and Phung, 2005). *B. licheniformis* is known to possess genes encoding ArsC (Corsini et al., 2010), while in literature there is no evidence about its ability to perform the As(V) dissimilatory reduction. For this reason, our discussion will be focused on ArsC-mediated As reduction.

As(V) reduction linked to detoxification processes is well explained in literature (Silver and Phung, 2005; Lloyd and Oremland, 2006). Briefly, As(V) chemically mimics phosphate, and it can enter the microbial cell by the pathways designated for phosphate uptake, interfering with phosphate-based biochemical pathways (e.g. oxidative phosphorylation). Bacteria developed a particular resistance to As which consists in the reduction of As(V) to As(III) with a specific cytoplasmatic protein ArsC (arsenate-reductase). Once As is reduced it is no more able to mimic phosphate and it is suitable to be excreted out of the cell via ArsB-type, As(III)-specific transport proteins (Oremland and Stolz, 2003; Silver and Phung, 2005).

In order to explain how As(III) uptake in calcite could take place, first of all it is worth mentioning again that As(III) is present only in bacterial calcite produced by *B. licheniformis* in a solid growth medium. *B. licheniformis* can reduce As(V) to As(III) by the ArsC pathway and then extrude As(III) in liquid growth medium (Tripti and Shardendu, 2016). The fate of As(III) can however be different in liquid and solid media, due mainly to two factors: rate of diffusion and biofilm structure.

We have already argued that a liquid medium allows for faster diffusion of As(V) (causing a higher As concentration in precipitated calcite) than a solid medium; it is likely that the same can be applicable for As(III) and oxygen. In the liquid medium, as long as swimming bacteria reduce As (V) to As(III), the availability of dissolved O_2 concentration could be high enough to re-oxidize As(III) to As(V). This could explain the absence of As(III) in calcite precipitated by bacterial activities in a liquid medium (LCC-Mg and LCC) as well as in Bullicame Travertines.

In a solid medium, in addition to the reduced diffusion of As and oxygen into the medium, bacteria can grow onto the surface where they are streaked (Figs. S2b–d), and quickly form thick external biofilms (at the solid-air interface) where individual cells are held together by a self-produced extracellular polymeric matrix or EPS (Branda et al., 2005). Diffusion limitation is well known to occur in biofilms (Stewart, 2003). So, biofilms would work as a barrier to the diffusion of oxygen from air to the cell surface and also of As(III), available at the bacterial cell surface by ArsB-mediated excretion, to the biofilm-air interface. This slow diffusion/-supply of As and oxygen can result in the entrapment of As(III) in the growing calcite inside the biofilm.

The proposed mechanism for As uptake by bacteria in the calcite grown in liquid and solid media is shown in Fig. 6. As(III) uptake in calcite can happen only in particular conditions, in which reduced diffusion or feeding rate of both As and O_2 is allowed, like a wetland environment. This could be the case of Pecora River Valley travertines which are mainly made up of "lacustrine and phytoclastic travertines" which actually host a calcite containing As (III) (Costagliola et al., 2010; Bardelli et al., 2011). On the contrary, LCC-Mg and LCC samples grown in the liquid culture media should resemble a hot spring environment with a continuous groundwater supply and relatively high fO_2, like Bullicame Hot Springs or others reported in literature (e.g. Winkel et al., 2013).

It should be noted that, besides slow diffusion, other processes, like organic complexation and organic coating, could preserve bacteria-extruded As(III) from oxidation. The same biofilm EPS could interact with As(III) and also entrap it into the matrix. The real mechanism relating this process is behind the aim of this work and will be likely investigated in future research.

Regarding the As uptake process in calcite, XAS data yield useful insights. Considering that adsorbed and co-precipitated As in calcite have distinct spectral patterns

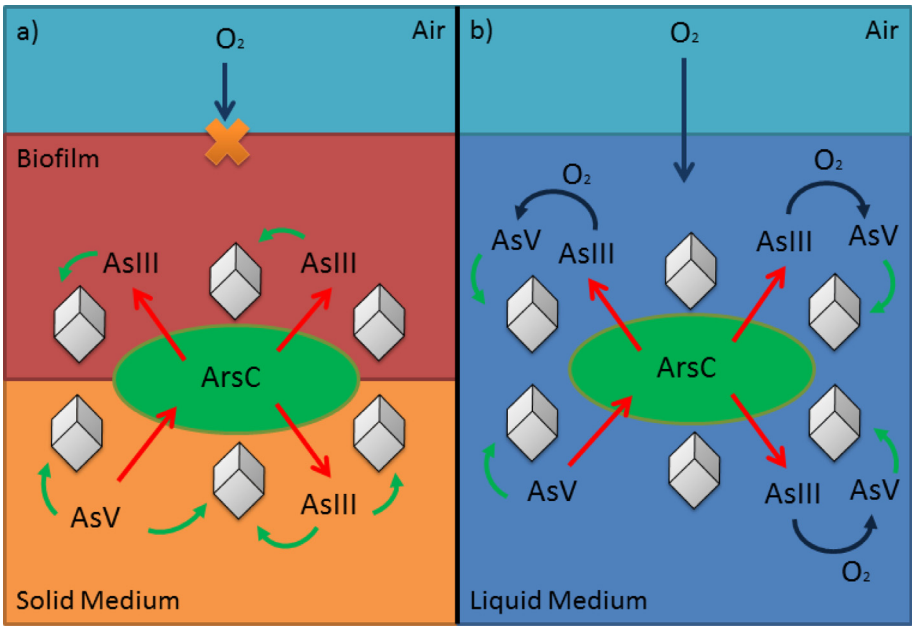

Fig. 6. Scheme of the bacterial As uptake process in solid (a) and liquid culture media (b). Bacteria are represented as green ellipse, while calcite as white rhombohedrons.

(Winkel et al., 2013), it seems clear that in Bullicame travertines (BL samples) co-precipitation of As in calcite is prevalent, while in ZIT and TRSE travertines adsorption onto mineral surfaces seems to be prevalent (Fig. 3), suggesting that in natural environments both the processes are allowed. In comparison, biogenic calcites LCC-Mg and LCC have an intermediate pattern, suggesting a commensurate effect of the two uptake processes. The As(III)-bearing biogenic sample, SCC-Mg, has an EXAFS very similar to liquid cultured ones, probably because of the low As(III) to As(V) molar ratio. SCC, on the contrary, exhibits a complex EXAFS spectrum, due to the presence of As with different oxidation states, and consequently different first coordination shells.

In any case, regardless of the uptake process, all samples show almost the same EXAFS spectral features (Fig. 5a) with a single-frequency oscillation, suggesting no contributions from coordination shells higher than the first (Bardelli et al., 2011). In fact, Fourier-Transformed spectra in R-Space exhibit a distinct first-shell coordination (1.23 Å before the phase shift correction), which corresponds to the As-O bonds of As(V) (estimated 1.69 Å). However, despite some slight differences in the Radial Distribution Function (RDF) from 2 to 6 Å, there is no evidence of a second coordination shell for As(III) nor for As(V)-bearing calcite. Such results clearly suggest that As uptake in biogenic calcite, just like in Bullicame travertines, happens without any ordering in calcite structure, regardless the uptake process and As speciation.

5. CONCLUSIONS

A multi-methodological characterization was performed on biogenic calcites produced by the As-resistant bacterium *B. licheniformis*, combining SEM imaging, X-ray Diffraction (XRD), X-ray Fluorescence (XRF), and X-ray Absorption Spectroscopy (XAS), in order to investigate the bio-mediated As uptake in calcite and point out the critical factors of this process.

The culture medium phase was noted to be a critical factor which strongly affects the phase composition of the biogenic products, the amount of As trapped in calcite and its oxidation state. In particular, our results suggest that in solid medium and in bacterial biofilm As diffusion is low, reflecting in a smaller apparent distribution coefficient, Kd (l/kg); oxygen diffusion from air is hindered, allowing the presence of As(III) in the precipitated calcite, starting from an As(V)-bearing solution.

This last issue is probably the most interesting outcome of this work. In fact it is known about the ability of bacteria to reduce As(V) to As(III) (Oremland and Stolz, 2003; Silver and Phung, 2005) and to precipitate calcite (Dhami et al., 2013), as long as the ability of calcite to sink As(V) (Winkel et al., 2013), but our results clearly demonstrate that the biogenic process could produce As(III)-bearing calcite. As(III) uptake in calcite has been widely debated in literature (Cheng et al., 1999; Román-Ross et al., 2006; Di Benedetto et al., 2006), but up until now no clear evidence has been reported in literature, with the only exception of Pecora Valley travertines reported by Bardelli et al. (2011), who argued about the possible role of bacteria in As(III) uptake in natural travertines. Our findings suggest that As(V) could have been reduced to As(III) by bacteria before its uptake in the calcite lattice. This is not a very common process in nature and probably it is confined to particular environments where the supply of As and oxygen is limited, like those where the travertine of the Pecora Valley formed.

Finally, our results suggest that the presence of Mg during calcite precipitation positively affects As uptake in calcite both in the chemical and bio-mediated process. Although this aspect goes beyond the scope of this work, our findings lead us to figure that As uptake induces a lattice distortion, reflecting in the elongation of c-axes, as asserted first by Cheng et al. (1999), while Mg induces a shrinking due to its shorter ionic radius. This "compensation" effect seems to positively affect As uptake in calcite, suggesting the use of Mg for As sequestration in calcite in biotechnological applications.

ACKNOWLEDGMENTS

X-ray absorption spectroscopy measurements were performed at GeoSoilEnviroCARS (The University of Chicago, Sector 13), Advanced Photon Source (APS), Argonne National Laboratory. GeoSoilEnviroCARS is supported by the National Science Foundation – Earth Sciences (EAR-16344415) and Department of Energy-GeoSciences (DE-FG02-94ER14466). This research, supported partially by the U.S. Department of Energy, Office of Basic Energy Sciences, Division of Chemical Sciences, Geosciences, and Biosciences through Argonne National Laboratory, used resources of the Advanced Photon Source, a U.S. Department of Energy (DOE) Office of Science User Facility operated for the DOE Office of Science by Argonne National Laboratory under Contract No. DE-AC02-06CH11357. The authors want to thank Dr. Roberta Faraone and Dr. Marco Coppi for their technical help in microbiological procedures, Dr. Samuele Ciattini (CRIST – University of Florence), Dr. Mario Paolieri, Dr. Maurizio Ulivi and Dr. Matteo Zoppi (Earth Sciences Dept. – University of Florence) for their support during the XRF, ICP-OES, SEM and XRD measurements. Finally, we want to thank Dr. Giuseppe Pagano, Mine Director of the Thermal Field of Viterbo, who allowed us to access to the hot springs.

APPENDIX A. SUPPLEMENTARY MATERIAL

Supplementary data associated with this article can be found, in the online version, at https://doi.org/10.1016/j.gca.2017.11.013.

REFERENCES

Achal V., Pan X., Fu Q. and Zhang D. (2012) Biomineralization based remediation of As(III) contaminated soil by *Sporosarcina ginsengisoli*. *J. Hazard. Mater.* **201–202**, 178–184.

Alexandratos V. G., Elziga E. J. and Reeder R. J. (2007) Arsenate uptake by calcite: macroscopic and spectroscopic characterization of adsorption and incorporation mechanisms. *Geochim. Cosmochim. Acta* **71**, 4172–4187.

Angelone M., Cremisini C., Piscopo V., Proposito M. and Spaziani F. (2009) Influence of hydrostratigraphy and structural setting on the arsenic occurrence in groundwater of the Cimino-Vico volcanic area (central Italy). *Hydrogeol. J.* **17**, 901–914.

Astilleros J., Fernández-Díaz L. and Putnis A. (2010) The role of magnesium in the growth of calcite: an AFM study. *Chem. Geol.* **271**, 52–58.

Barabesi C., Galizzi A., Mastromei G., Rossi M., Tamburini E. and Perito B. (2007) *Bacillus subtilis* gene cluster involved in calcium carbonate biomineralization. *J. Bacteriol.* **189**(1), 228–235.

Bardelli F., Benvenuti M., Costagliola P., Di Benedetto F., Lattanzi P., Meneghini C., Romanelli M. and Valenzano L. (2011) Arsenic uptake by natural calcite: an XAS study. *Geochim. Cosmochim. Acta* **75**, 3011–3023.

Branda S. S., Vik S., Friedman L. and Kolter R. (2005) Biofilms: the matrix revisited. *Trends Microbiol.* **13**, 20–26.

Castanier S., Métayer-Levrel L. and Perthuisot J.-P. (1999) Ca-carbonates precipitation and limestone genesis – the microbiologist point of view. *Sed. Geol.* **126**, 9–23.

Chakraborty S., Bardelli F., Mullet M., Greneche J.-M., Varma S., Ehrhardt J.-J., Banerjee D. and Charlet L. (2011) Spectroscopic studies of arsenic retention onto biotite. *Chem. Geol.* **281**, 83–92.

Cheng L., Fenter P., Sturchio N. C., Zhong Z. and Bedzyk M. J. (1999) X-ray standing wave study of arsenite incorporation at the calcite surface. *Geochim. Cosmochim. Acta* **63**(19/20), 3153–3157.

Corsini A., Cavalca L., Crippa L., Zaccheo P. and Andreoni V. (2010) Impact of glucose on microbial community of a soil containing pyrite cinders: role of bacteria in arsenic mobilization under submerged condition. *Soil Biol. Biochem.* **42**, 699–707.

Costagliola P., Benvenuti M. M., Benvenuti M. G., Di Benedetto F. and Lattanzi P. (2010) Quaternary sediment geochemistry as a proxy for toxic element source: a case study of arsenic in the Pecora Valley (southern Tuscany, Italy). *Chem. Geol.* **270**(1–4), 80–89.

Costagliola P., Bardelli F., Benvenuti M., Di Benedetto F., Lattanzi P., Romanelli M., Paolieri M., Rimondi V. and Vaggelli G. (2013) Arsenic-bearing calcite in natural travertines: evidence from sequential extraction, μXAS, and μXRF. *Environ. Sci. Technol.* **47**, 6231–6238.

Dhami N. K., Reddy M. S. and Mukherjee A. (2013) Biomineralization of calcium carbonates and their engineered applications: a review. *Front. Microbiol.* **4**, 1–13.

Di Benedetto F., Costagliola P., Benvenuti M., Lattanzi P., Romanelli M. and Tanelli G. (2006) Arsenic incorporation in natural calcite lattice: evidence from electron spin echo spectroscopy. *Earth Planet. Sci. Lett.* **246**, 458–465.

Di Benedetto F., Montegrossi G., Minissale A., Pardi L. A., Romanelli M., Tassi F., Delgado Huertas A., Pampin E. M., Vaselli O. and Borrini D. (2011) Biotic and inorganic control on travertine deposition at Bullicame 3 spring (Viterbo, Italy): a multidisciplinary approach. *Geochim. Cosmochim. Acta* **75**, 4441–4455.

Dixit S. and Hering J. G. (2003) Comparison of arsenic(V) and arsenic(III) sorption onto iron oxide minerals: implications for arsenic mobility. *Environ. Sci. Technol.* **37**, 4182–4189.

Finch A. A. and Allison N. (2007) Coordination of Sr and Mg in calcite and aragonite. *Mineral. Mag.* **71**(5), 539–552.

Fortin D., Ferris F. G. and Beveridge T. J. (1997) Surface-mediated mineral development by bacteria. *Rev. Mineral.* **35**, 161–180.

Fukushi K., Sakai M. and Munemoto T. (2011) Arsenic sorbent for remediating arsenic-contaminated material. *US Patent* No: 8,227,378.

Graf D. L. (1961) Crystallographic tables for the rhombohedral carbonates. *Am. Miner.* **46**, 1283–1316.

Han Y.-J. and Aizenberg J. (2003) Effect of magnesium ions on oriented growth of calcite on carboxylic acid functionalized self-assembled monolayer. *J. Am. Chem. Soc.* **125**, 4032–4033.

Kamiya N., Kagi H., Tsunomori F., Tsuno H. and Notsu K. (2004) Effect of trace lanthanum ion on dissolution and crystal growth of calcium carbonate. *J. Cryst. Growth* **267**, 635–645.

Konhauser K. (2007) *Introduction to Geomicrobiology*. Blackwell Science Ltd., pp. 73–74.

Krysiak A. and Karczewska A. (2007) Arsenic extractability in soils in the areas of former arsenic mining and smelting, SW Poland. *Sci. Total Environ.* **379**, 190–200.

Lenoble V., Bouras O., Deluchat V., Serpaud B. and Bollinger J. C. (2002) Arsenic adsorption onto pillared clays and iron oxides. *J. Colloid Interface Sci.* **255**(1), 52–58.

Lloyd J. R. and Oremland R. S. (2006) Microbial transformations of arsenic in the environment: from soda lakes to aquifers. *Elements* **2**, 85–90.

Markgraf S. A. and Reeder R. J. (1985) High-temperature structure refinements of calcite and magnesite. *Am. Miner.* **70**, 590–600.

Marvasi M., Vedovato E., Balsamo C., Macherelli A., Dei L., Mastromei G. and Perito B. (2009) Bacterial community analysis on the Mediaeval stained glass window "Natività" in the Florence Cathedral. *J. Cult. Heritage* **10**, 24–133.

Matschullat J. (2000) Arsenic in the geosphere – a review. *Sci. Total Environ.* **249**, 297–312.

Murcott S. (2012) *Arsenic Contamination in the World: An International Sourcebook*. IWA Publishing, London, UK.

Nriagu J. O. (1994) *Arsenic in the Environment. Part I: Cycling and Characterization*. John Wiley & Sons, INC, New York.

Ogino T., Suzuki T. and Sawada K. (1987) The formation and transformation mechanism of calcium carbonate in water. *Geochim. Cosmochim. Acta* **51**, 2757–2767.

Oremland R. S. and Stolz J. F. (2003) The ecology of arsenic. *Science* **300**, 939–944.

Oremland R. S., Stolz J. F. and Hollibaugh J. T. (2004) The microbial arsenic cycle in Mono Lake, California. *FEMS Microbiol. Ecol.* **48**(2004), 15–27.

Ouvrard S., De Donato P., Simonnot M. O., Begin S., Ghanbaja J., Alnot M., Duval Y. B., Lhote F., Barres O. and Sardin M. (2005) Natural manganese oxide: combined analytical approach for solid characterization and arsenic retention. *Geochim. Cosmochim. Acta* **69**, 2715–2724.

Paquette J. and Reeder R. J. (1990) Single-crystal X-ray structure refinements of two biogenic magnesian calcite crystals. *Am. Miner.* **75**, 1151–1158.

Perito B. and Mastromei G. (2011) Molecular basis of bacterial calcium carbonate precipitation. In *Molecular Biomineralization, Aquatic Organisms Forming Extraordinary Materials* (ed. W. E. G. Müller). Springer Verlag, Berlin, Heidelberg, pp. 113–139.

Perito B., Marvasi M., Barabesi C., Mastromei G., Bracci S., Vendrell M. and Tiano P. (2014) A *Bacillus subtilis* cell fraction (BCF) inducing calcium carbonate precipitation: biotechnological perspectives for monumental stone reinforcement. *J. Cult. Heritage* **15**, 345–351.

Pokroy B., Fitch A. N., Marin F., Kapon M., Adir N. and Zolotoyabko E. (2008) Anisotropic lattice distortions in biogenic calcite induced by intra-crystalline organic molecules. *J. Struct. Biol.* **155**, 96–103.

Ravel B. and Newville M. (2005) ATHENA, ARTEMIS, HEPHAESTUS: data analysis for X-ray absorption spectroscopy using IFEFFIT. *J. Synchrotron Radiat.* **12**, 537–541.

Raven K. P., Jain A., Raven R. H. L., Jain K. P. A. and Loeppert R. H. (1998) Arsenite and arsenate adsorption on ferrihydrite: kinetics, equilibrium, and adsorption envelopes. *Environ. Sci. Technol.* **32**, 344–349.

Román-Ross G., Cuello G. J., Turrillas X., Fernández-Martìnez A. and Charlet L. (2006) Arsenite sorption and co-precipitation with calcite. *Chem. Geol.* **233**, 328–336.

Sherman D. and Randal S. (2003) Surface complexation of arsenic (V) to iron(III) (hydr)oxides: structural mechanism from ab initio molecular geometries and EXAFS spectroscopy. *Geochim. Cosmochim. Acta* **67**(22), 4223–4230.

Silver S. and Phung Le T. (2005) Genes and enzymes involved in bacterial oxidation and reduction of inorganic arsenic. *Appl. Environ. Microbiol.* **71**(2), 599–608.

Smedley P. L. and Kinniburgh D. G. (2002) A review of the source, behaviour and distribution of arsenic in natural waters. *Appl. Geochem.* **217**, 517–568.

Sø H. U., Postma D., Jakobsen R. and Larsen F. (2008) Sorption and desorption of arsenate and arsenite on calcite. *Geochim. Cosmochim. Acta* **72**, 5871–5884.

Stewart P. S. (2003) Diffusion in biofilms. *J. Bacteriol.* **185**, 1485–1491.

Toby B. H. (2001) EXPGUI, a graphical user interface for GSAS. *J. Appl. Crystallogr.* **34**, 210–213.

Tripti K. and Shardendu S. (2016) PH modulates arsenic toxicity in *Bacillus licheniformis* DAS-2. *Ecotoxicol. Environ. Saf.* **130**, 240–247.

Tufano K. T., Reyes C. W., Saltikov C. and Fendorf S. (2008) Reductive processes controlling arsenic retention: revealing the relative importance of iron and arsenic reduction. *Environ. Sci. Technol.* **42**, 8283–8289.

Vahabi A., Ramezanianpour A. A., Sharafi H., Zahiri H. S., Vali H. and Noghabi K. A. (2013) Calcium carbonate precipitation by strain *Bacillus licheniformis* AK01, newly isolated from loamy soil: a promising alternative for sealing cement-based materials. *J. Basic Microbiol.* **53**, 1–7.

Veith B., Herzberg C., Steckel S., Feesche J., Maurer K. H., Ehrenreich P., Bäumer S., Henne A., Liesegang H., Merkl R., Ehrenreich A. and Gottschalk G. (2004) The complete genome sequence of *Bacillus licheniformis* DSM13, an organism with great industrial potential. *J. Mol. Microbiol. Biotechnol.* **7**(4), 204–211.

Warren L. A., Maurice P. A., Parmar N. and Ferris F. (2001) Microbially mediated calcium carbonate precipitation: implications for interpreting calcite precipitation and for solid-phase capture of inorganic contaminants. *Geomicrobiol J.* **18**(1), 93–115.

Weisener C. G., Guthrie J. W., Smeaton C. M., Paktunc D. and Fryer B. J. (2011) The effect of Ca–Fe–As coatings on microbial leaching of metals in arsenic bearing mine waste. *J. Geochem. Explor.* **110**, 23–30.

Winkel L. H. E., Casentini B., Bardelli F., Voegelin A., Nikolaidis N. P. and Charlet L. (2013) Speciation of arsenic in Greek travertines: co-precipitation of arsenate with calcite. *Geochim. Cosmochim. Acta* **106**, 99–110.

Yokoyama Y., Tanaka K. and Takahashi Y. (2012) Differences in the immobilization of arsenite and arsenate by calcite. *Geochim. Cosmochim. Acta* **91**, 202–219.

Zolotoyabko E., Caspi E. N., Fieramosca J. S., Von Dreele R. B., Marin F., Mor G., Addadi L., Weiner S. and Politi Y. (2010) Differences between bond lengths in biogenic and geological calcite. *Cryst. Growth Des.* **10**(3), 1207–1214.

Associate editor: Hailiang Dong